VILNIUS UNIVERSITY

Žilvinas Ledas

COMPUTATIONAL MODELLING OF THE SELF-ORGANIZATION OF LUMINOUS BACTERIA IN LIQUID

Summary of a doctoral dissertation
Physical sciences, informatics (09 P)

Vilnius, 2016

The doctoral dissertation was written in 2011–2015 at Vilnius University Faculty of Mathematics and Informatics.

Scientific supervisor:

Prof. Dr. Romas Baronas (Vilnius University, Physical Sciences, Informatics – 09 P).

The dissertation will be defended at the Council of Scientific Field of Informatics at Vilnius University:

Chairman:

Prof. Dr. Habil. Gintautas Dzemyda (Vilnius University, Physical Sciences, Informatics – 09 P).

Members:

Prof. Dr. Habil. Mindaugas Bloznelis (Vilnius University, Physical Sciences, Informatics – 09 P),

Dr. Mindaugas Radžiūnas (Weierstrass Institute for Applied Analysis and Stochastics, Leibniz Institute in Forschungsverbund Berlin e. V., Physical Sciences, Informatics – 09 P).

Prof. Dr. Habil. Minvydas Kazys Ragulskis (Kaunas University of Technology, Physical Sciences, Informatics – 09 P),

Prof. Dr. Julius Žilinskas (Vilnius University, Physical Sciences, Informatics – 09 P),

The dissertation will be defended at the open meeting of the Council of Scientific Field of Informatics at Vilnius University Faculty of Mathematics and Informatics on June 6, 2016 at 1 PM. Address: Didlaukio g. 47, LT-08303 Vilnius, Lithuania.

The summary of the dissertation was distributed on May 6, 2016.

The doctoral dissertation is available at the library of Vilnius University and at VU webpage: *www.vu.lt/lt/naujienos/ivykiu-kalendorius*

Doctoral dissertation was supported by the Research Council of Lithuania (LMT Grant No. MIP-001/2014).

VILNIAUS UNIVERSITETAS

Žilvinas Ledas

KOMPIUTERINIS ŠVYTINČIŲJŲ BAKTERIJŲ STRUKTŪROS FORMAVIMOSI TIRPALE MODELIAVIMAS

Daktaro disertacijos santrauka
Fiziniai mokslai, informatika (09 P)

Vilnius, 2016

Disertacija parengta 2011–2015 metais Vilniaus universiteto Matematikos ir informatikos fakultete.

Mokslinis vadovas:

prof. dr. Romas Baronas (Vilniaus universitetas, fiziniai mokslai, informatika – 09 P)

Disertacija ginama Vilniaus universiteto Informatikos mokslo krypties taryboje:

Pirmininkas:

prof. habil. dr. Gintautas Dzemyda (Vilniaus universitetas, fiziniai mokslai, informatika – 09 P).

Nariai:

prof. habil. dr. Mindaugas Bloznelis (Vilniaus universitetas, fiziniai mokslai, informatika – 09 P),

dr. Mindaugas Radžiūnas (Vejerštraso taikomosios analizės ir stochastikos institutas Berlyne, fiziniai mokslai, informatika – 09 P).

prof. habil. dr. Minvydas Kazys Ragulskis (Kauno technologijos universitetas, fiziniai mokslai, informatika – 09 P),

prof. dr. Julius Žilinskas (Vilniaus universitetas, fiziniai mokslai, informatika – 09 P),

Disertacija ginama viešame Informatikos mokslo krypties tarybos posėdyje 2016 m. birželio mėn. 6 d. 13 val. Vilniaus universiteto Matematikos ir informatikos fakultete, Didlaukio g. 47, LT-08303, Vilnius, Lietuva.

Disertacijos santrauka išsiųsta 2016 m. gegužės mėn. 6 d.

Disertaciją galima peržiūrėti Vilniaus universiteto bibliotekoje ir VU interneto svetainėje adresu: *www.vu.lt/lt/naujienos/ivykiu-kalendorius*

Disertacijos rengimas paremtas Lietuvos mokslo tarybos (LMT grant No. MIP-001/2014).

Introduction

Research context and motivation

Various microorganisms respond to certain chemicals found in their environment by migrating towards higher or lower concentrations of the substance. Such directed movement is called chemotaxis [12], which plays a crucial role in a wide range of biological phenomena, e.g., within the embryo, chemotaxis affects avian gastrulation and patterning of the nervous system [11, 31].

Bacterial growth and movement in confined suspensions often results in the emergence of patterns [3]. The interaction of several active processes in the living suspensions leads to very complex dynamic systems which are still poorly understood [6].

Recently, the dynamics of *Escherichia coli* cultures was investigated using bioluminescence imaging [34, 36]. Moreover, lux-gene engineered bacteria have been successfully used to develop whole cell biosensors, which have been successfully used for the detection of environmental pollutants [13].

Computational modelling can be applied to validate biological results retrospectively and to develop new hypothesis. Because such modelling employs nonlinear equations, the only suitable way to solve them is numerical simulation [32].

Aim and tasks of the research

The aim of this work was to create a flexible computational model for self-organization of bacteria, which could be successfully used to model results obtained in physical experiments, and to investigate peculiarities of bacterial population dynamics by applying the model. The aim is further divided into the following tasks:

1. Create a flexible computational model suitable for modelling self-organization of bacterial population using simple enough expressions (following Hillen and Painter [14], hereinafter referred to as “minimal”).
2. Mathematically model the effect of oxygen on the pattern formation of bacterial population.
3. Tune up the created model to match results obtained in physical experiments.
4. Generalize the created model for two- and three-dimensional space and analyse numerical simulation results in one-, two- and three-dimensions.
5. Develop software tools to facilitate the processing and visualization of modelled results or results produced by luminous bacteria in physical experiments.
6. Using the developed software, investigate the peculiarities and behaviour of the results modelled and results produced by luminous bacteria in physical experiments.

Research methods

The mathematical models presented in this thesis are formulated by nonlinear reaction-diffusion partial differential equations. The models were approximated employing a finite difference technique by applying an explicit computational scheme. Software tools implementing computational schemes were developed using Free Pascal.

Additional software tools were developed to facilitate the processing and visualization of modelled results or results produced by luminous bacteria in physical experiments. A video game engine was used for 3D visualization. These tools were used to investigate the peculiarities of the modelled results.

Scientific novelty and results

1. The model (referred to as "minimal") suitable for modelling pattern formation in a luminous *E. coli* colony in pseudo-one dimension along the three-phase contact line was selected.
2. Mathematical and computational models suitable for modelling pattern formation in a luminous *E. coli* colony in two and three dimensions of space were created. The added equation describing oxygen dynamics ensures that computationally simulated structures better match results obtained in physical experiments.
3. It was shown that dynamics of bacterial patterns can be computationally simulated with reduced spatial dimensions in a model (by using 1D and 2D models instead of 3D). Moreover, it was shown that important changes in the patterns are observed when using models with reduced spatial dimensions and the same parameter values.

Practical significance of the results

The mathematical models presented and proposed in this thesis are used to model and investigate results of pattern formation in a luminous *E. coli* colony obtained from bioluminescence imaging.

The following software was created:

1. Software implementing mathematical models used to investigate bacterial behaviour.
2. Software "E. Coli Image Analysis"[1] which facilitates processing, analysis and comparison of results.

[1] This software can be found at *http://uosis.mif.vu.lt/~zledas/bakt/ImageAnalysis/*.

3. Unity game engine (version 4.6) was adapted to be used for the visualization of 3D modelling results.

The results presented in this thesis were used for reaching the goals of the project "Self-organization of *E. coli* and their mutants near three phase contact line" financed by the Research Council of Lithuania (MIP-001/2014).

Statements promoted to defend

1. The selected model (referred to as "minimal") is suitable for modelling pattern formation in a luminous *E. coli* colony in pseudo-one dimension along the three-phase contact line.
2. When equation describing oxygen dynamics is added, mathematical and computational models become suitable for modelling pattern formation in a luminous *E. coli* colony in two and three dimensions of space in the case when a vessel with depth needs to be modelled.
3. Dynamics of bacterial patterns can be computationally simulated with reduced spatial dimensions in a model (using 1D and 2D models instead of 3D), but important changes in the patterns are observed when using models with the same parameter values in different dimensions.

Approbation of the results

The main research results were published in five articles in periodical scientific publications [A2–A6]. Three of these articles were published in the journals with the citation index in Thomson Reuters Web of Science database [A2, A5, A6]. The contribution of the author of the thesis in the published papers covers the development of numerical models and the software solving these models, digital investigation processes, analysis of the results and varying in scope text preparation process. Also, part of the research results were published in peer reviewed conference proceedings [A1]. Contributed talks were given at seven international and national conferences.

1. Previous work

1.1. Mathematical and computational modelling

In the last decades computational modelling became to be intensively used for modelling physical and biological processes. Such modelling applications aim to transfer real world processes to abstract mathematical models and using computational approximations solve them in the end obtaining new knowledge and insights regarding real world processes [17, 27].

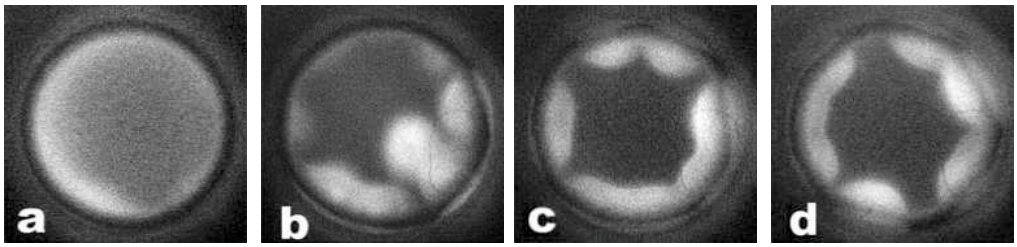

1 pav. Top view bioluminescent *E. coli* images of the bacterial cultures in a cylindrical vessel (bright color shows higher concentration). The images were captured at 5 (a), 20 (b), 40 (c), 60 (d) min. [36].

These computational simulations help to understand processes, which are very expensive or next to impossible to replicate in real life.

1.2. Chemotaxis and spatiotemporal patterns

Various microorganisms respond to certain chemicals found in their environment by migrating towards higher (chemoattraction) or lower (chemorepulsion) concentrations of the substance. The directed movement of microorganisms in response to chemical gradients is called chemotaxis [12]. Chemotaxis plays a crucial role in a wide range of biological phenomena, e.g., within the embryo: it affects avian gastrulation and the patterning of the nervous system [11, 31].

Although chemotaxis has been observed in many bacterial species, *Escherichia coli* is one of the widely studied examples. *E. coli* responds to the chemical stimulus by alternating the rotational direction of their flagella [12, 41]. Usually, microorganisms (including *E. coli*) not only move towards a chemoattractant, but they also produce more of the chemoattractant. Because of this, the motile microorganisms aggregate into local clusters with a high density and hence produce pattern formation [3, 4, 27].

Recently, the spatiotemporal patterns in the fluid cultures of *E. coli* have been observed by employing lux-gene engineered cells and a bioluminescence imaging technique [34, 36]. However, mechanisms governing the formation of bioluminescence patterns remain unclear.

Photographs of luminous *E. coli* taken at different time moments can be seen in Fig. 1 (taken from the top) [36] and Fig. 2 (taken from the side). Moreover, the space-time plot of bioluminescent *E. coli* measured along the contact line of the cylindrical vessel is presented in Fig. 3 ([35, 36]). It can be seen from these images that patterns formed by luminous bacteria as well as their dynamics are complex. The patterns evolve over time – high concentration areas emerge, move and merge.

Over the last two decades, lux-gene engineered bacteria have been used to develop whole cell-based biosensors [10]. A whole-cell biosensor is an analyte probe

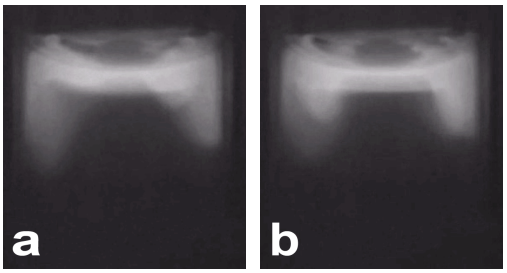

2 pav. Side view bioluminescent *E. coli* images of the bacterial cultures in a cylindrical glass vessel (bright color shows higher concentration). The images were captured at two different moments. The author of the images: Dr. Remigijus Šimkus.

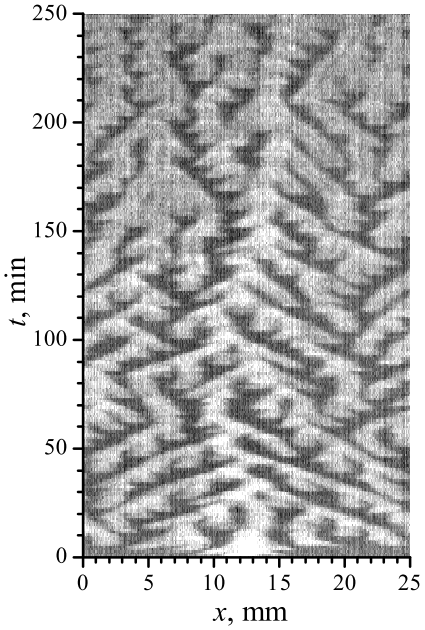

3 pav. Space-time plot of bioluminescent *E. coli* measured along the contact line of the cylindrical vessel (bright color shows higher concentration) [35, 36].

consisting of a biological element, eg. genetically engineered bacteria, integrated with an electronic component to yield a measurable signal [24]. Such devices have been successfully used for the detection of environmental pollutant bioavailability, various stressors, including dioxins, endocrine-disrupting chemicals, and ionizing radiation [13].

To solve the problems currently limiting the practical use of whole-cell biosensors, the bacterial self-organization within the biosensors has to be comprehensively investigated.

1.3. Mathematical modelling of chemotaxis

Starting with the first works of Keller and Segel [18], mathematical modelling plays a crucial role in understanding the mechanisms of chemotaxis [14]. Different mathematical models based on advection-reaction-diffusion equations have been developed for computational modelling of pattern formation in bacterial colonies [3, 4, 6, 22, 25]. The system of coupled nonlinear partial differential equations introduced by Keller and Segel are still among the most widely used [14, 18, 29].

According to the Keller and Segel approach, the main biological processes can be described by a system of two conservation equations ($t > 0$),

$$\begin{aligned} \frac{\partial n}{\partial t} &= \nabla \left(D_n \nabla n - h(n,c) n \nabla c \right) + f(n,c), \\ \frac{\partial c}{\partial t} &= \nabla \left(D_c \nabla c \right) + g_p(n,c) n - g_d(n,c) c, \end{aligned} \tag{1}$$

where x and t stand for space and time, $n(x,t)$ is the cell density, $c(x,t)$ is the chemoattractant concentration, $D_n(n)$ and D_c are the diffusion coefficients, $f(n,c)$ stands for cell growth and death, $h(n,c)$ stands for the chemotactic sensitivity, g_p and g_d describe the production and degradation of the chemoattractant [18].

1.3.1. Cell kinetics

The cell growth $f(n,c)$ is usually assumed to be a logistic function,

$$f(n,c) = k_1 n \left(1 - \frac{n}{n_0} \right), \tag{2}$$

where k_1 is the constant growth rate of the cell population [4].

1.3.2. Chemoattractant production and consumption

Various chemoattractant production functions have been used in chemotactic models [14]. Usually, a saturating function of the cell density is used indicating that, as the cell density increases, the chemoattractant production decreases. The Michaelis-Menten function is widely used to express the production rate g_p [18, 25, 28],

$$g_p(n,c) = \frac{k_2}{k_3 + n}, \tag{3}$$

and the degradation or consumption g_d of the chemoattractant is typically constant,

$$g_d(n,c) = k_4. \tag{4}$$

The values of k_2, k_3 and k_4 are not exactly known yet.

1.3.3. Chemotactic sensitivity

The function $h(n, c)$ controls the chemotactic response of the cells to the chemoattractant. The signal-dependent sensitivity and the density-dependent sensitivity are the two main kinds of the chemotactic sensitivity $h(n, c)$ [14]. In order to reproduce the experimentally observed bands Keller and Segel introduced a chemotactic (signal-dependent) sensitivity of the following form [19]:

$$h(n, c) = \frac{k_5}{c}. \tag{5}$$

Since the bacterial current flow declines at low chemical concentrations and saturates at high concentrations, Lapidus and Schiller derived the "receptor" chemotactic (signal-dependent) sensitivity for *E. coli* [22],

$$h(n, c) = \frac{k_6}{(k_7 + c)^2}. \tag{6}$$

Assuming that cells carry a certain finite volume, a density-dependent chemotactic sensitivity function as well as a volume-filling model were derived by Hillen and Painter [30],

$$h(n, c) = k_8 \left(1 - \frac{n}{n_0}\right). \tag{7}$$

Another form for the density-dependent chemotactic sensitivity has been introduced by Velazquez [39],

$$h(n, c) = \frac{k_9}{k_{10} + n}. \tag{8}$$

In the simplest form, chemotactic sensitivity is assumed to be independent of the chemoattractant concentration c, and the cell density n, i.e., $h(n, c)$ can be constant, $h(n, c) = k_8$.

1.3.4. Linear and nonlinear diffusion

Both diffusion coefficients (D_n and D_c) are usually assumed to be constant. However, the nonlinear cell diffusion depending on the chemoattractant concentration or/and the cell density is also considered [14]. The nonlinear diffusion of this form can be used

$$D_n(n) = D_n \left(\frac{n}{n_0}\right)^m, \tag{9}$$

where n_0 is the maximal density (or carrying capacity) of the cell population ($n < n_0$) [20]. At $m < 0$ the rate of diffusion increases as the cell density increases, while at $m > 0$ the rate decreases as the cell density increases. Assuming $m = 0$ leads to a constant rate of the cell diffusion.

1.3.5. Local and non-local gradient

E. coli is able to detect a gradient by sampling the chemoattractant concentration over the time and adjusting their movement accordingly. As a result, the signal detected by the cell is non-local and the non-local gradient can be used to model this behaviour [15],

$$\overset{\circ}{\nabla}_{\rho} c(x,t) = \frac{n}{|S^{n-1}|\,\rho} \int_{S^{n-1}} \sigma c(x+\rho\sigma, t) d\sigma, \tag{10}$$

where S^{n-1} denotes the $(n-1)$-dimentional unit sphere in $\mathbb{R}^n$ and ρ is the sampling radius. When $\rho \to 0$, this model becomes an ordinary model with local sampling.

1.3.6. Linear and nonlinear gradient

Linear dependency on chemoattractant gradient means that unlimited cell speeds are possible and this is unrealistic. To solve it, the nonlinear gradient function F_{ς} (such that when $\varsigma \to 0$ becomes a linear gradient) can be used [14].

1.3.7. General and minimal models

Replacing f, g_p, g_d, D_n and ∇c with the concrete expressions above, and using the nonlinear gradient function F_{ς}, the governing equations (1) are reduced to a cell kinetics model with the nonlinear signal kinetics; the nonlinear cell diffusion; the nonlinear chemotactic sensitivity; the non-local sampling and non-local gradient,

$$\begin{aligned} \frac{\partial n}{\partial t} &= D_n \nabla \left(\left(\frac{n}{n_0} \right)^m \nabla n \right) - \\ &\quad - \nabla \left(h(n,c) n \mathrm{F}_{\varsigma} \left(\overset{\circ}{\nabla}_{\rho} c \right) \right) + k_1 n \left(1 - \frac{n}{n_0} \right), \\ \frac{\partial c}{\partial t} &= D_c \Delta c + \frac{k_2 n}{k_3 + n} - k_4 c, \quad x \in (0,l), \quad t > 0, \end{aligned} \tag{11}$$

where Δ is the Laplace operator formulated in the one-dimensional Cartesian coordinate system, and l is the length of the contact line, i.e., the circumference of the vessel. Assuming R as the vessel radius, $l = 2\pi R$, $x \in (0, 2\pi R)$.

According to the model classification by Hillen and Painter, the dimensional model (11) is comprised of the signal-dependent sensitivity (M2); the density-dependent sensitivity (M3); the non-local sampling (M4); the nonlinear diffusion (M5); the saturating signal production (M6); the nonlinear gradient (M7) and the cell kinetics (M8) models [14]. On the other hand, when using simple function forms and dropping cell kinetics, a minimal model M1 is derived [14]:

$$\begin{aligned} \frac{\partial n}{\partial t} &= \nabla \left(D_n \nabla n - h n \nabla c \right), \\ \frac{\partial c}{\partial t} &= D_c \Delta c + n - c, \quad x \in (0,l), \quad t > 0, \end{aligned} \tag{12}$$

where h is constant chemotactic sensitivity.

1.3.8. Initial and boundary conditions

Different boundary conditions can be used in the modelling, eg., no-flux [14, 29] or periodicity [1, 35]. To the system of previously described equations, periodicity boundary ($t > 0$)

$$\begin{aligned} n(0,t) = n(l,t), \quad & \left.\frac{\partial n}{\partial x}\right|_{x=0} = \left.\frac{\partial n}{\partial x}\right|_{x=l}, \\ c(0,t) = c(l,t), \quad & \left.\frac{\partial c}{\partial x}\right|_{x=0} = \left.\frac{\partial c}{\partial x}\right|_{x=l}, \end{aligned} \tag{13}$$

and initial ($t = 0$) conditions

$$n(x,0) = n_{0x}(x), \quad c(x,0) = 0, \quad x \in [0,l], \tag{14}$$

are added. Here $n_{0x}(x)$ is the initial ($t = 0$) non uniform bacterial concentration.

1.3.9. General dimensionless model

In order to define the main governing parameters of the mathematical model (11)-(13), a dimensionless mathematical model has been derived by introducing the following dimensionless parameters [14, 27, 28]:

$$\begin{aligned} & u = \frac{n}{n_0}, \quad v = \frac{k_3 k_4 c}{k_2 n_0}, \quad t^* = \frac{k_4 t}{s}, \quad x^* = \sqrt{\frac{k_4}{D_c s}}x, \quad D = \frac{D_n}{D_c}, \\ & \alpha_u = \frac{k_1}{k_4}, \quad \beta_v = \frac{n_0}{k_3}, \quad \rho^* = \frac{\rho}{l}, \quad \chi(u,v) = \frac{k_2 n_0}{k_3 k_4 D_c} h(n_0 u, k_2 n_0 c/(k_3 k_4)). \end{aligned} \tag{15}$$

Dropping the asterisks, the dimensionless governing equations become ($t > 0$)

$$\begin{aligned} \frac{\partial u}{\partial t} = & \frac{\partial}{\partial x}\left(D u^m \frac{\partial u}{\partial x}\right) - \frac{\partial}{\partial x}\left(\chi(u,v) u \mathrm{F}_\varsigma\left(\mathring{\nabla}_\rho\, v\right)\right) + \\ & + s\alpha_u u(1-u), \\ \frac{\partial v}{\partial t} = & \frac{\partial^2 v}{\partial x^2} + s\left(\frac{u}{1+\beta_v u} - v\right), \quad x \in (0,1), \end{aligned} \tag{16}$$

where x and t stand for the dimensionless space and time, respectively; u is the dimensionless cell density; v is the dimensionless chemoattractant concentration; α_u is the dimensionless growth rate of the cell population; β_v stands for the saturating of the signal production; $\chi(u,v)$ is the dimensionless chemotactic sensitivity; and s stands for the spatial and temporal scale.

Assuming the one-dimensional Cartesian coordinate system the non-local gradient can be described as [14]:

$$\mathring{\nabla}_\rho\, v(x,t) = \frac{v(x+\rho,t) - v(x-\rho,t)}{2\rho}. \tag{17}$$

The nonlinear gradient in a dimensionless form can be expressed as [14]:

$$\mathrm{F}_\varsigma(\nabla v) = \frac{1}{\varsigma}\tanh\left(\frac{\varsigma\nabla v}{1+\varsigma}\right), \tag{18}$$

where ς describes nonlinear gradient strength.

For the dimensionless simulation of the spatiotemporal pattern formation in a luminous *E. coli* colony, four forms of the chemotactic sensitivity function $\chi(u,v)$ were used to find out the best fitting pattern for the experimental data [34–36],

$$\chi(u,v) = \frac{\chi_0}{(1+\chi_\alpha v)^2}, \tag{19a}$$

$$\chi(u,v) = \chi_0\frac{1+\chi_\beta}{v+\chi_\beta}, \tag{19b}$$

$$\chi(u,v) = \chi_0\left(1-\frac{u}{\chi_\gamma}\right), \tag{19c}$$

$$\chi(u,v) = \frac{\chi_0}{1+\chi_\epsilon u}. \tag{19d}$$

The first two forms (19a) and (19b) of the function $\chi(u,v)$ correspond to the signal-dependent sensitivity, while the other two (19c) and (19d) – for the density-dependent sensitivity [14]. Assuming that $\chi_\alpha = 0$, $\chi_\beta \to \infty$, $\chi_\gamma \to \infty$ or $\chi_\epsilon = 0$ it leads to a constant form of the chemotactic sensitivity, $\chi(u,v) = \chi_0$.

The boundary conditions (13) transform to the following dimensionless equations ($t > 0$):

$$\begin{aligned} u(0,t) &= u(1,t), \quad \left.\frac{\partial u}{\partial x}\right|_{x=0} = \left.\frac{\partial u}{\partial x}\right|_{x=1}, \\ v(0,t) &= c(1,t), \quad \left.\frac{\partial v}{\partial x}\right|_{x=0} = \left.\frac{\partial v}{\partial x}\right|_{x=1}. \end{aligned} \tag{20}$$

The initial conditions (14) take the following dimensionless form:

$$\begin{aligned} u(x,0) &= 1+\varepsilon(x), \\ v(x,0) &= 0, \quad x \in [0,1], \end{aligned} \tag{21}$$

where $\varepsilon(x)$ is a random spatial perturbation.

1.4. Numerical simulation

Computational methods are the only possible way to solve the complex problems presented in this thesis as no analytical solution is possible because of the nonlinearity of the governing equations of the models [27, 32].

One of the widely used methods suitable for the problems encountered in this thesis is the finite difference method [7, 21, 32]. In case of the finite difference method,

finite differences are used to approximate the derivatives in the mathematical models. Then a digital simulator must be used to solve the approximated problem.

Various finite difference methods exist, but the most commonly used in the computational modelling are explicit and various implicit schemes. An explicit finite difference scheme is obtained by applying left-handed approximation of the first time derivative. It is simple to implement and has relatively low computational costs, because it gives value of the solution for the new time step explicitly in terms of values at the previous time step. This method was used in this thesis.

2. Mathematical modelling of a luminous bacterial self-organization

Firstly, the bacterial self-organization model suitable for modelling in 1D is presented in this chapter. Then, the original 2D model with the added oxygen dynamics equation is proposed [A4–A6]. Finally, generalization of this proposed model for 2D and 3D dimensions is presented [A2].

2.1. Modelling of a bacterial self-organization along the contact line

In this work the spatiotemporal pattern formation in the fluid cultures of luminous *E. coli* placed in a rounded glass container is investigated. The container is modelled by a right circular cylinder as shown in Fig. 4, where r and h are the base radius and the height of the cylinder, respectively. For simplicity, it was assumed that the fluid fills the container. Assuming the direct proportionality between bioluminescence and the number of active cells, a bacterial self-organization can be modelled by the dynamics of the density of bioluminescent cells [35].

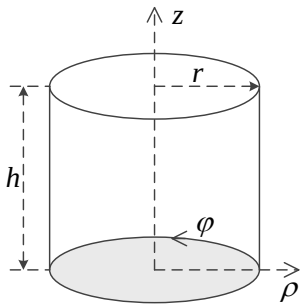

4 pav. The principal structure of a rounded container.

Investigating the density of bioluminescent cells in a circular cylinder container, it is visible that high density areas are concentrated along top contact line [34, 36]. As a result, it is possible to project density of the top contact line onto 1D spatiotemporal plot as in Fig. 2.

Mathematical and computational models suitable for modelling such 1D spatiotemporal plots of *E. coli* were proposed in [1, 35]. They can be expanded with additional modifications. The extended mathematical model was described as (11)-(13), with a corresponding dimensionless model (16), (21), (20).

2.2. Modelling of a bacterial self-organization on the lateral surface

The minimal model (34) determined in this work is adjusted in this section to be suitable for modelling the lateral surface of the cylinder.

The model is based on the equations where reaction term incorporates the carrying capacity. By some interpretations [A5] the carrying capacity can be restrained by the availability of oxygen. Because it is not known how the carrying capacity is dependent on resource availability, two options are considered:

1. Carrying capacity is not dependent on (O_2) concentration.
2. Carrying capacity is linearly dependent on (O_2) concentration.

This further outlined model was originally developed by the author of this thesis with co-authors [A5].

2.2.1. Model with the constant carrying capacity

The processes taking place in a colony of *E. coli* near the cylinder lateral surface when it is assumed that there is no relationship between growth and oxygen concentration was described by a system of two equations, which in the dimensionless form reads [1, 35]

$$\begin{aligned} \frac{\partial u}{\partial t} &= D\Delta u - \chi\nabla\left(u\nabla v\right) + s\alpha_u u\left(1-u\right), \\ \frac{\partial v}{\partial t} &= \Delta v + s\left(\frac{u}{1+\beta_v u} - v\right), \end{aligned} \tag{22}$$

where Δ is the Laplace operator in the Decartes coordinate system; x and y stands for the dimensionless space; t is the dimensionless time; $u(x, y, t)$ denotes the dimensionless active cell density; $v(x, y, t)$ denotes the dimensionless chemoattractant concentration; D describes the cell diffusivity; χ – is the chemotactic sensitivity; α_u – is the dimensionless growth rate of an active cell population; β_v – stands for the saturating signal production; and s stands for the spatial and temporal scale [14, 29]. By complementing the (22) system with initial and boundary conditions (not shown here) we get the model that can be used to model cells in 2D.

2.2.2. Model with the resource (oxygen) dependent carrying capacity

Aiming to simulate the patterns, including space-plots near the contact line and snapshots of the cell density near the inner lateral surface, more comparable to the patterns observed in the experiments, the two-dimensional model (22) was extended by introducing the oxygen dynamics equation:

$$\begin{aligned}\frac{\partial u}{\partial t} &= D\Delta u - \chi\nabla\left(u\nabla v\right) + s\alpha_u u\left(1-\frac{u}{o}\right),\\ \frac{\partial v}{\partial t} &= \Delta v + s\left(\frac{u}{1+\beta_v u} - v\right),\\ \frac{\partial o}{\partial t} &= D_o\Delta o - s\lambda u,\end{aligned} \tag{23}$$

where $o(x, y, t)$ is the concentration of oxygen; D_o denotes the dimensionless oxygen diffusivity; λ stands for the dimensionless consumption rate of oxygen; and the meaning of the remaining parameters is the same as in (22). By complementing (23) with initial and boundary conditions we get the model that is suitable for modelling the case where oxygen diffuses into the system at the top surface, cells consume oxygen and in this way their carrying capacity is restrained by availability of oxygen.

2.3. Model generalization to two and three dimensions

In most cases the investigation of dynamics of *E. coli* cultures are restricted to one (1D) or two (2D) dimensions in space. Recently, three-dimensional (3D) aggregation patterns based on the volume-filling Keller-Segel model have been studied numerically, and new patterns called P-surfaces, perforated lamellar, completely specific to 3D have been obtained [33]. The 3D simulation was also applied to investigate the activity-induced phase separation in concentrated suspensions of active particles, and important differences between the 2D and 3D cases were found [37].

In the next subsections of this section the generalized 3D model of the bacterial self-organization suitable for simulating spatiotemporal patterns in the fluid cultures of luminous *E. coli* in a rounded container is presented.

Since the simulation based on the 3D model is very time-consuming, therefore reducing spatial dimensionality in a model for simulating 1D and 2D spatiotemporal patterns was investigated.

2.3.1. Governing equations

According to the model extension described in Subsection 2.2.2, adding an additional equation to dimensional equations (1) and inserting concrete expressions to the system, leads to the following governing equations of the population kinetics

model:

$$\begin{aligned}
\frac{\partial n}{\partial t} &= D_n \Delta n - \nabla \left(k_1 n \nabla c\right) + k_2 n \left(1 - \frac{n}{k_3 s}\right), \\
\frac{\partial c}{\partial t} &= D_c \Delta c + \frac{k_4 n}{k_5 + n} - k_6 c, \\
\frac{\partial s}{\partial t} &= D_s \Delta s - k_7 n, \quad \mathrm{x} \in \Omega, \quad t > 0,
\end{aligned} \tag{24}$$

where Δ is the Laplace operator; x and t stand for space and time, m denotes dimensionality of the space; $s(\mathrm{x}, t)$ is the concentration of a nutrient; D_s is the diffusion coefficient usually assumed to be constant; k_1 is the chemotactic sensitivity; k_2 is the growth rate of the cell population; k_3 stands for the cell density under steady-state conditions; k_4 and k_5 stand for saturating chemoattractant production; k_6 and k_7 are the consumption rates of the chemoattractant and the nutrient, respectively; the other notations are the same as in the model (1).

Assuming the rounded container as a right circular cylinder, the mathematical model in the cylinder at the domain Ω can be defined in cylindrical coordinates,

$$\mathrm{x} = (\rho, \varphi, z), \quad \Omega = (0, r) \times (0, 2\pi) \times (0, h), \tag{25}$$

where r and h are the base radius and the height of the cylinder Ω as shown in Fig. 4.

2.3.2. Dimensionless model

To reduce the number of the main governing parameters of (24), a dimensionless model can be derived by setting

$$\begin{aligned}
&u = \frac{n}{n_0}, \quad v = \frac{k_5 k_6 c}{k_4 n_0}, \quad o = \frac{k_3 s}{n_0}, \\
&t^* = k_6 t, \quad \rho^* = \sqrt{\frac{k_6}{D_c}}\rho, \quad \varphi^* = \varphi, \quad z^* = \sqrt{\frac{k_6}{D_c}} z, \\
&D_u = \frac{D_n}{D_c}, \quad D_o = \frac{D_s}{D_c}, \quad \chi = \frac{k_1 k_4 n_0}{k_5 k_6 D_c}, \quad \alpha_u = \frac{k_2}{k_6}, \quad \beta_v = \frac{n_0}{k_5}, \quad \gamma_o = \frac{k_7 k_3}{k_6},
\end{aligned} \tag{26}$$

where n_0 is the cell density under steady state conditions. When modelling the carrying capacity by a linear function of the nutrient concentration ($k_3 s$), the cell density under steady state conditions is directly proportional to the concentration s_0 of the nutrient near the top surface, $n_0 = k_3 s_0$.

Dropping the asterisks, the dimensionless governing equations then become

$$\begin{aligned}
\frac{\partial u}{\partial t} &= D_u \Delta u - \chi \nabla \left(u \nabla v\right) + \alpha_u u \left(1 - \frac{u}{o}\right), \\
\frac{\partial v}{\partial t} &= \Delta v + \frac{u}{1 + \beta_v u} - v, \\
\frac{\partial o}{\partial t} &= D_o \Delta o - \gamma_o u, \quad (\rho, \varphi, z) \in (0, R) \times (0, 2\pi) \times (0, H), \quad t > 0.
\end{aligned} \tag{27}$$

where u is the dimensionless cell density; v is the dimensionless chemoattractant concentration; o is the dimensionless concentration of the nutrient; α_u is the dimensionless growth rate of the cell population; β_v stands for saturating of the signal production; γ_o is dimensionless consumption rate of the nutrient; R and H are the relative radius and height of the cylinder: $R = r\sqrt{k_6/D_c}$, $H = h\sqrt{k_6/D_c}$.

2.3.3. Population dynamics near the top surface

The bacterial self-organization near the inner top surface of a rounded container can be modelled by applying the common 3D mathematical model (24) as well as the corresponding dimensionless model (27) However, transient computational simulations based on 3D mathematical models are extremely time and resource consuming. The dimension reduction is a widely used approach to increase efficiency of the numerical simulation [38].

When modelling the bacterial self-organization near the top surface of a right circular container, the mathematical model can be defined in the polar coordinates on a 2D domain – a circle [A1]. Due to a constant concentration of the nutrient near the top surface, the dynamics of the nutrient concentration can be ignored.

Due to modelling the carrying capacity by a linear function of the nutrient concentration ($k_3 s$ in (24)) and the assumption $n_0 = k_3 s_0$, the term $k_2 n(1 - n/(k_3 s))$ of the logistic cell growth is reduced to $k_2 n(1 - n/n_0)$, while the corresponding dimensionless term $\alpha_u u(1 - u/o)$ approaches $\alpha_u u(1 - u)$. The dynamics of the bacterial population near the top surface of a right circular container can be described by the following governing equations formulated in polar coordinates:

$$\begin{aligned} \frac{\partial u}{\partial t} &= D_u \Delta u - \chi \nabla \left(u \nabla v\right) + \alpha_u u \left(1 - u\right), \\ \frac{\partial v}{\partial t} &= \Delta v + \frac{u}{1 + \beta_v u} - v, \quad (\rho, \varphi) \in (0, R) \times (0, 2\pi), \quad t > 0, \end{aligned} \tag{28}$$

where Δ is the Laplace operator in the polar coordinates ρ and φ, u and v are functions of the two parameters ρ and φ.

2.3.4. Population dynamics near the three-phase contact line

When observing the patterns of inhomogeneous bioluminescence in small cylindrical containers, the bioluminescence images of bacterial cultures showed an accumulation of luminous bacteria near the three-phase contact line Fig. 1 and Fig. 2, and [34, 36]. Such dynamics of the bacterial population near the three-phase contact line can be modelled also by applying the common 3D mathematical model (27) (assuming $\rho = R$, $z = H$) as well as the 2D mathematical model (28) (assuming $\rho = R$). However, the dimension of these models could be reduce to one.

The dynamics of the bacterial population near the circumference of the top surface of right circular cylinder can be approximated by the following governing

equations formulated in one polar coordinate φ,

$$\begin{aligned}\frac{\partial u}{\partial t} &= D_u \frac{1}{R^2}\frac{\partial^2 u}{\partial \varphi^2} - \chi \frac{1}{R^2}\frac{\partial}{\partial \varphi}\left(u\frac{\partial v}{\partial \varphi}\right) + \alpha_u u\,(1-u)\,,\\ \frac{\partial v}{\partial t} &= \frac{1}{R^2}\frac{\partial^2 v}{\partial \varphi^2} + \frac{u}{1+\beta_v u} - v, \quad \varphi \in (0, 2\pi), \quad t > 0,\end{aligned} \tag{29}$$

where u and v are functions of one space parameter φ and one time parameter t.

The 1D mathematical model (29) can be reformulated by replacing the azimuth parameter φ with the longitudinal parameter x by applying $x = \varphi R$,

$$\begin{aligned}\frac{\partial u}{\partial t} &= D_u \frac{\partial^2 u}{\partial x^2} - \chi \frac{\partial}{\partial x}\left(u\frac{\partial v}{\partial x}\right) + \alpha_u u\,(1-u)\,,\\ \frac{\partial v}{\partial t} &= \frac{\partial^2 v}{\partial x^2} + \frac{u}{1+\beta_v u} - v, \quad x \in (0, L), \quad t > 0,\end{aligned} \tag{30}$$

where u and v are functions of one parameter x. L is the dimensionless length of the contact line, i.e. the circumference of the vessel (a circle), $L = 2\pi R = 2\pi r\sqrt{k_6/D_c}$, where r is dimensional radius of the base of the cylinder as shown in Fig. 4.

The mathematical model (30) has been successfully used to study the bacterial self-organization of luminous *E. coli* along the contact line of a circular container [1, 9, 35]. Here this model was shown to be a very special case of the common 3D mathematical model (27).

2.3.5. Population dynamics near the lateral surface

The dynamics of the bacterial population near the lateral surface can be modeled by applying the common 3D model (27) (assuming $\rho = R$). The radial transport of cells, chemoattractant and nutrient can be ignored because of the zero flux condition at the lateral surface ($\rho = R$ in the model (27)).

The dynamics of the bacterial population near the lateral surface of a cylinder can approximately be described using equations (27) and by replacing parameter ρ with a constant R and assuming that functions u, v and o have only two parameters φ and z. Since the lateral surface of a right circular cylinder is a rectangle, the corresponding mathematical model could be defined in the Cartesian coordinates system.

The bacterial self-organization near the lateral surface can be defined in the Cartesian system in the same manner as (27) with the adjusted domain and Laplace

operator,

$$\begin{aligned}
\frac{\partial u}{\partial t} &= D_u \left(\frac{\partial^2 u}{\partial x^2} + \frac{\partial^2 u}{\partial z^2} \right) - \chi \left(\frac{\partial}{\partial x} \left(u \frac{\partial v}{\partial x} \right) + \frac{\partial}{\partial z} \left(u \frac{\partial v}{\partial z} \right) \right) + \alpha_u u \left(1 - \frac{u}{o} \right), \\
\frac{\partial v}{\partial t} &= \frac{\partial^2 v}{\partial x^2} + \frac{\partial^2 v}{\partial z^2} + \left(\frac{u}{1 + \beta_v u} - v \right), \\
\frac{\partial o}{\partial t} &= D_o \left(\frac{\partial^2 o}{\partial x^2} + \frac{\partial^2 o}{\partial z^2} \right) - \gamma_o u, \quad (x, z) \in (0, L) \times (0, H), \quad t > 0.
\end{aligned} \tag{31}$$

where u, v and o are the functions of the parameters x and z; L is the dimensionless circumference of the cylinder base and H is the dimensionless height of the cylinder: $L = 2\pi R = 2\pi r\sqrt{k_6/D_c}$, $H = h\sqrt{k_6/D_c}$.

A 2D model (23) that was described in Subsection 2.2 used the dimensionless space and time scaling parameter s. This parameter is used by some authors [25] and not used by others [14]. It is worth mentioning that the s parameter can be introduced to the equations described in this section by applying transformation:

$$t^* = \frac{t}{s}, \quad \rho^* = \frac{\rho}{\sqrt{s}}, \quad z^* = \frac{z}{\sqrt{s}}, \tag{32}$$

Here it was shown that the 2D model described in Subsection 2.2 matches the model (31) described in this subsection and is a special case of the common 3D mathematical model (27).

3. Solving the mathematical models and additional software tools

Software for the computational model of the bacterial self-organization and methods employed for reducing the time needed for computational modelling is presented in the first part of this chapter. Then, additional software for processing of experimental data and visualizing 3D modelling results is described.

3.1. Software for the computational model of the bacterial self-organization

Computational methods are the only possible way to solve the complex problems presented in this thesis as no analytical solution is possible because of the nonlinearity of the governing equations of the models [27, 32]. Therefore, computational model was derived from the presented models by using a finite difference technique and applying the explicit computational scheme [7, 21, 32].

A software tool implementing computational schemes was developed using Free Pascal [23]. It allows choosing a desired model from the predefined 1D, 2D and 3D model set with the desired initial conditions and other model parameters.

3.2. Reducing the time needed for computational modelling

Computational modelling in 2D and 3D can take a long time (from a dozen of minutes to a few days) so it is important to explore options for reducing this time. By employing two methods described further, the time required for modelling in 3D using the model (27) was reduced from 8.9 to 3.2 days.

When modelling computationally, the grid with mesh points distributed with constant step sizes along all space dimensions is usually used [32]. The investigated 2D polar (28) and 3D (27) models in φ dimension use step size h_φ which tends to decrease when approaching the centre of the circle. Using this property it is possible to use variable step size h_φ. The optimisation was implemented in the software employed for computational modelling to use a bigger step size when approaching the centre of the circle. Such optimisation yielded in a reduced number of computational operations by 31.25%, which in turn reduced the duration of the modelling by a similar amount.

Another way to reduce the duration of the modelling is to employ various parallel algorithms [8, 40]. It is not so difficult to parallelize explicit finite difference scheme calculations by dividing the space domain into sections and solving those sections separately for each time step. Threads were used to implement such parallelization [8] in the calculations of previously described software. Barriers were used to synchronise the threads [40].

Theoretically it is possible to reduce the duration of the process by half when using two threads instead of one, but an acceleration of 1.56-1.64 was achieved in real calculations. This is due to the fact that not all operations were parallelized. The highest acceleration of 1.91 was achieved for 3D model using four threads.

3.3. Additional software for the processing of experimental data and visualizing 3D modelling results

A software called "E. Coli Image Analysis"[2] with two main functions was developed:

1. To load animated images, mark the places of the vessels and extract pseudo-one dimensional spatiotemporal plots from the loaded 2D images (Fig. 5, left).

2. To load pseudo-one dimensional spatiotemporal plots and to isolate and count high concentration areas (Fig. 5, right). This function uses signal processing techniques to extract brighter areas in the images. This function can be used on simulated as well as on real experiment data to have a kind of objective pattern similarity measure.

[2]This software can be found at *http://uosis.mif.vu.lt/~zledas/bakt/ImageAnalysis/*.

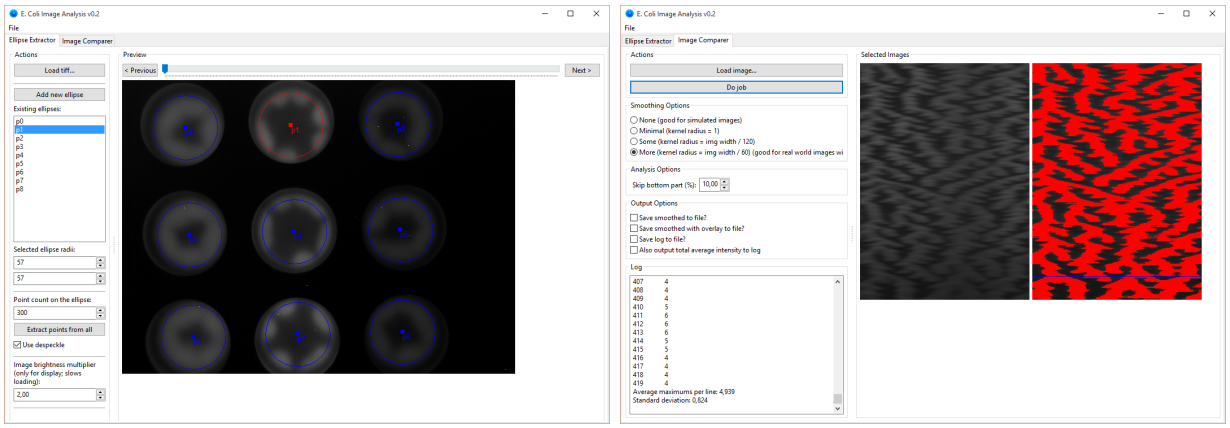

5 pav. Left: pseudo-one dimensional spatiotemporal plot extraction from 2D photos. Right: Isolating and counting high concentration areas in a pseudo-one dimensional plot.

Lazarus integrated development environment [5] and Free Pascal were used to develop this software.

Additionally, as the real-time visualization of changing in time 3D modelling results would be very convenient, the Unity game engine (version 4.6) [2] was adapted to be used for the visualization of such results (first two images of Fig. 11).

4. Investigation of the peculiarities of modelled results and comparison with results obtained in physical experiments

In the first sections of this chapter, variations of the model are investigated in order to determine an appropriate minimal model [A1, A3]. Then, oxygen dynamics is added to the model and its influence on bacterial patterns is explored [A4–A6]. Finally, model generalization to two and three dimensions is investigated [A2].

4.1. Modelling of bacterial self-organization in a circular container along the contact line

The aim of the work presented in this section was to improve the already existing computational model by introducing additional modifications, specifically the nonlinear diffusion of cells, the non-local sampling, several kinds of chemotactic sensitivity and nonlinear gradient [14].

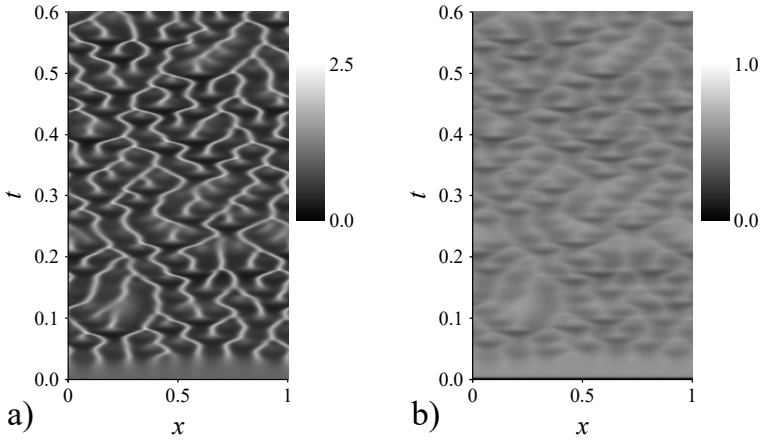

6 pav. Simulated space-time plots of the dimensionless cell density u (a) as well as the chemoattractant concentration v (b). Values of the parameters are as defined in (33).

4.1.1. Numerical simulation

The digital simulator described in Section 3.1 was used. By varying the model parameters the simulation results were analyzed with a special emphasis on achieving a spatiotemporal pattern similar to the experimentally obtained shown in Fig. 3. Fig. 6 shows the results of the informal pattern fitting, where Fig. 6a and Fig. 6b present the simulated space-time plots of the dimensionless cell density u and the chemoattractant concentration v, respectively.

Regular oscillations as well as chaotic fluctuations similar to the experimental ones were computationally simulated. Assuming the constant form of the chemotactic sensitivity ($\chi(u, v) = \chi_0$) and a simple gradient, the dynamics of the bacterial population was simulated at the following values of the model parameters [35]:

$$\begin{aligned} &D = 0.1, \quad \chi_0 = 6.2, \quad \rho = 0, \quad \alpha_u = 1, \\ &\beta_v = 0.73, \quad s = 625, \quad m = 0. \end{aligned} \tag{33}$$

A spatially-varying random perturbation $\varepsilon(x)$ of the dimensionless cell density u with an average of 1 and a standard deviation of 0.1 was applied to the initial distribution of bacteria.

Due to a relatively great number of model parameters, there is no guarantee that the values (33) mostly approach the pattern shown in Fig. 3. Similar patterns were achieved at different values of the model parameters. An increase in one parameter can be often compensated by decreasing or increasing another one. Because of this, it is important to investigate the influence of the model parameters on the pattern formation and to develop a mathematical model containing a minimal number of parameters [1, 14, 29].

4.1.2. Results of numerical simulation and discussion

By varying the input parameters the output results were analyzed with a special emphasis on the influence of chemotactic sensitivity, a non-local gradient and diffusion nonlinearity on the spatiotemporal pattern formation in the luminous *E. coli* colony. Fig. 6a shows the spatiotemporal pattern for the constant form of the chemotactic sensitivity ($\chi(u,v)=\chi_0$) applying a simple gradient ($\varsigma\to\infty$ and $\rho\to 0$) and the linear diffusion ($m=0$).

The effects of the different chemotactic sensitivity functions were investigated assuming the linear diffusion ($m=0$) and a simple gradient ($\varsigma\to\infty$ and $\rho\to 0$). The non-local gradient and the nonlinear diffusion were analyzed separately and together assuming constant chemotactic sensitivity and the linear gradient ($\chi(u,v)=\chi_0$ and $\varsigma\to\infty$). The nonlinear gradient and the nonlinear diffusion were analyzed separately and together assuming the constant chemotactic sensitivity and the local gradient ($\chi(u,v)=\chi_0$ and $\rho\to 0$).

Signal-dependent sensitivity was computationally modelled by two forms of the chemotactic sensitivity function $\chi(u,v)$: (19a) and (19b). The spatiotemporal patterns of the dimensionless cell density u were simulated at very different values of χ_α and χ_β.

Assuming $\chi_\alpha=0$ or $\chi_\beta\to\infty$, leads to a signal-independence, i.e., a constant form, of the chemotactic sensitivity, $\chi(u,v)=\chi_0$. The results of the multiple simulations showed that the simulated patterns differ from the experimental ones when increasing the χ_α-parameter or decreasing the χ_β-parameter. Because of this, there is no practical reason for applying a non-constant form of the signal-dependent sensitivity and it can be ignored when modelling the pattern formation in a luminous *E. coli* colony.

Two forms, (19c) and (19d), of **chemotactic sensitivity** function $\chi(u,v)$ were employed for the computational modelling of the density-dependent chemotactic sensitivity. The spatiotemporal patterns of the cell density u were simulated at various values of χ_γ ir χ_ϵ.

Assuming $\chi_\gamma\to\infty$ or $\chi_\epsilon=0$, leads to a density-independence, i.e., a constant form, of chemotactic sensitivity, $\chi(u,v)=\chi_0$. Multiple simulation showed that the simulated patterns differ from the experimental ones when decreasing the χ_γ-parameter or increasing the χ_ϵ-parameter.

Because of this, there is no practical reason for the application of a non-constant form of the density-dependent sensitivity when modelling the pattern formation in a colony of luminous *E. coli* and a simple constant form ($\chi(u,v)=\chi_0$) of chemotactic sensitivity can be successfully applied to modelling the formation of the bioluminescence patterns in a colony of luminous *E. coli*.

The non-local sampling was modelled by using non-local gradient (17). The constant chemotactic sensitivity ($\chi(u,v)=\chi_0$) was used in these simulations. The spatiotemporal patterns of the dimensionless cell density u were simulated at various values of the effective sampling radius ρ.

Assuming $\rho = 0$, leads to a model with the local sampling and the simple gradient, the operator $\overset{\circ}{\nabla}_\rho$ approaches ∇. The computational results showed that the simulated patterns get dissimilar from the experimental ones when increasing the ρ-parameter. It was seen from the results that merging of different "branches" in the pattern is almost gone and this merging behaviour is essential to get patterns similar to experimental ones. Because of this, there is no practical reason to apply the non-local gradient to modelling the formation of the patterns in a colony of luminous *E. coli*.

The nonlinear diffusion was modelled by using the following form of the diffusion function $D(u) = u^m$ [20]. Chemotactic sensitivity was assumed to be constant ($\chi(u, v) = \chi_0$) in these simulations. The spatiotemporal patterns of the dimensionless cell density u were simulated at various values of m-parameter.

Assuming $m = 0$, leads to a model with linear diffusion. The results of the simulations at different m values show that patterns tend to drift away from the experimental ones when increasing ($m \to \infty$) or decreasing ($m \to -\infty$) the m-parameter. Some simulated patterns contain fewer mergers of different "branches" (as a result of $m \ll 0$), and others exhibit the "branch" movements that are distorted compared to the experimentally observed ones (as a result of $m \gg 0$). Therefore, there is no need to use the nonlinear diffusion for modelling the pattern formation in a colony of luminous *E. coli*.

The nonlinear gradient was modeled by using (18). Chemotactic sensitivity was assumed to be constant ($\chi(u, v) = \chi_0$) in these simulations. The spatiotemporal patterns of the dimensionless cell density u were simulated at various values of the ς-parameter.

Assuming $\varsigma \to 0$, leads to a model with a linear gradient. The results of the simulations at different ς values show that patterns tend to drift away from the experimental ones when increasing the ς-parameter. The simulated patterns contain considerably fewer mergers of different "branches" or none at all. Therefore, there is no need to use a nonlinear gradient for modelling the pattern formation in a colony of luminous *E. coli*.

From the simulations with the non-local gradient and the nonlinear diffusion it was seen that the increasing the non-local gradient parameter ρ has a visually opposite effect to the increasing nonlinear diffusion parameter m. A similar observation was made regarding the nonlinear gradient and the nonlinear diffusion – it was seen that the increase of the nonlocal gradient parameter ς has visually opposite effect to the increasing nonlinear diffusion parameter m.

As a result, additional numerical experiments were carried out to determine how these combinations affect the pattern formation. Experiments did not confirm that the models with the non-local sampling and the nonlinear diffusion or the nonlinear gradient and the nonlinear diffusion are capable to produce a result that better matches the experimentally observed one. Because of this, there is no practical need to apply these modifications for the computational modelling of the pattern formation in a colony of luminous *E. coli*.

4.1.3. A minimal model suitable for the modelling of bacterial self-organization in 1D

In the previous subsections it was shown that the pattern formation along the contact line in a cellular population can be modelled at the following values of the model parameters: $m = 0$, $\chi_\alpha = 0$, $\chi_\beta \to \infty$, $\chi_\gamma \to \infty$, $\chi_\epsilon = 0$, $\varsigma \to 0$. Assuming these values leads to a reduction of the governing equations (16) to the following form:

$$\begin{aligned} &\frac{\partial u}{\partial t} = D\frac{\partial^2 u}{\partial x^2} - \chi_0 \frac{\partial}{\partial x}\left(u\frac{\partial v}{\partial x}\right) + s\alpha_u u(1-u), \\ &\frac{\partial v}{\partial t} = \frac{\partial^2 v}{\partial x^2} + s\left(\frac{u}{1+\beta_v u} - v\right), \\ &x \in (0,1), \quad t > 0. \end{aligned} \tag{34}$$

According to the classification of the chemotaxis models introduced by Hillen and Painter [14], the minimal model (34) is a combination of two models: the nonlinear signal kinetics model M6 and the cell kinetics model M8. This combination of the models has comprehensively been analyzed by Maini and others [25, 27, 28].

4.2. Modelling of the population dynamics near the lateral surface of a cylinder

The 2D model suitable for modelling bacterial population dynamics near the lateral surface will be investigated in this section.

4.2.1. The case of the constant carrying capacity

The length of the lateral surface of the cylinder assumed to be 1 and $h = 0.3$ because of the same proportions used in real world experiments. Time was $T = 0.7$. Other parameter values were the same or similar to the ones used previously (33) [1, 35]:

$$\begin{aligned} &D = 0.04, \quad \chi = 8.3, \quad \alpha_u = 1, \quad \beta_v = 0.73, \\ &s = 600, \quad h = 0.3, \quad T = 0.7. \end{aligned} \tag{35}$$

Mathematically, the simulations of quasi-one dimensional patterns of bioluminescence, which are seen from above by the two-dimensional model (22) imply the summation of luminous cells along the y coordinate. However, real suspension is turbid and inhomogeneous. It is clear that the detected light intensity depends on the depth of the layer from which the bioluminescence originates. The qualitative incorporation of this dependence was provided by assuming that the bioluminescence is proportional to the number of active cells which are above the level of $y = h - h_0, 0 < h_0 <= h$, where h_0 is the thickness of the experimentally "detectable" layer.

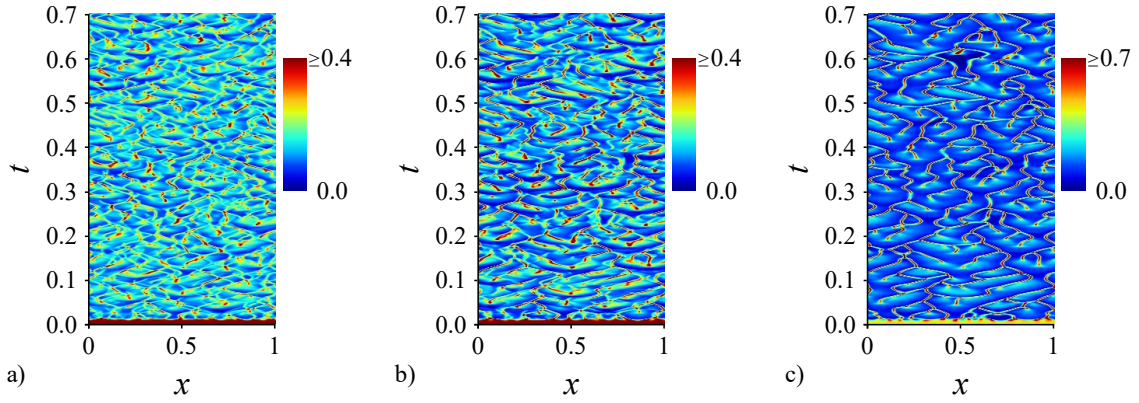

7 pav. Space-time plots of the cell density u_{1D} calculated along the three-phase contact line using (35) parameter values, and three heights of the detectable bioluminescence: $h_0 = h$ (a), $h_0 = 0,5h$ (b) ir $h_0 = 0,1h$ (c).

To simulate the spatiotemporal patterns seen from above (Fig. 2 and Fig. 3) by applying the two-dimensional model (22), the density of active cells was integrated over the detectable layer of the culture and then averaged,

$$u_{1D}(x,t) = \frac{1}{h_0}\int_{h-h_0}^{h} u(x,y,t)\,\mathrm{d}y, \quad x \in [0,1],\ t \in [0,T]. \tag{36}$$

Examples of the simulated spatiotemporal patterns are shown in Fig. 7. The density $u_{1D}(x,t)$ of the cells was calculated for different depths h_0 of the integration layer. As one can see from Fig. 3 and Fig. 7, the two-dimensional model based on (22) simulates quite well the pattern formation along the three-phase contact line when the thin detectable layer is assumed ($h_0 \to 0$) (Fig. 7c). The patterns obtained when integrating over the entire depth (Fig. 7a) are rather different from the pattern seen in the experiment (Fig. 3). It should also be noted that the decrease in the depth of the detectable layer ($h_0 \to 0$) implies the one-dimensional modelling of the pattern formation.

The dynamics of the number of aggregates formed in a spatiotemporal pattern is one of the most important characteristics of the patterns representing the self-organization of a bacterial population [29]. Two average numbers μ_x and μ_t of aggregates and the corresponding standard deviations σ_x and σ_t were calculated along the three-phase contact line and during the population evolution, respectively. The software tool described in Section 3.3 was used to make calculations.

These averaged μ_x and μ_t values with the corresponding σ_x and σ_t values were used to compare the similarity of two or more patterns. These values for the relevant images are summarized in Table 1.

By applying the two-dimensional model (22) the active cell densities along the wall of a tube were calculated. A typical example of simulated lateral patterns of

1 lentelė The average numbers μ_x and μ_t of aggregates and the corresponding standard deviations σ_x and σ_t calculated for the spatiotemporal patterns depicted in the relevant figures.

Figure	μ_x	σ_x	μ_t	σ_t
Fig. 3	5.98	0.91	10.08	1.80
Fig. 7a	10.64	1.98	31.30	4.02
Fig. 7b	8.38	1.62	25.82	3.74
Fig. 7c	7.02	1.09	19.58	3.46
Fig. 9a	6.59	0.92	10.00	1.54
Fig. 9b	6.57	0.92	9.96	1.56
Fig. 9c	6.64	0.99	9.83	1.65

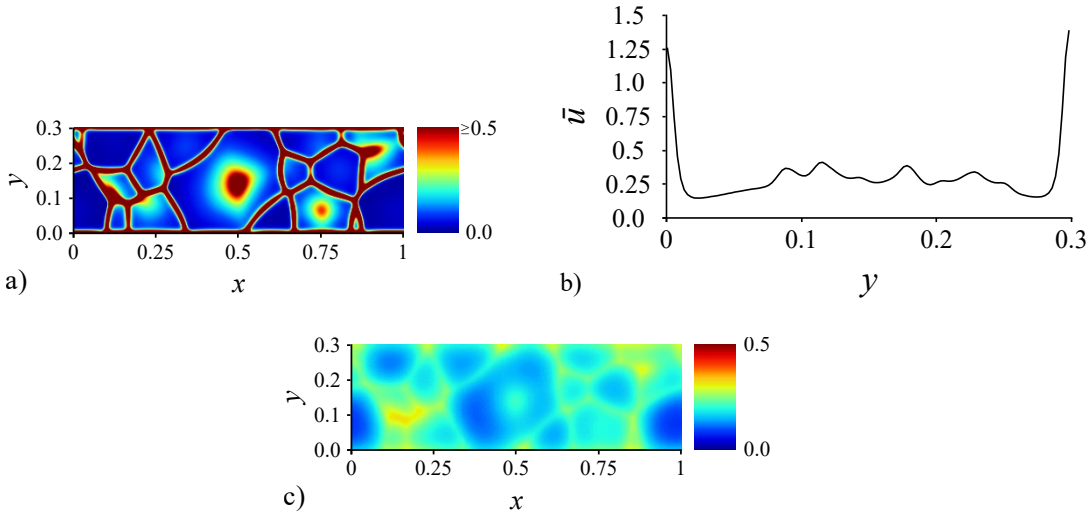

8 pav. Snapshots of the cell density u (a) and the chemoattractant concentration v (c) on the inner lateral surface of the tube and the profile of the vertical distribution of cells (b) at $t = 0.4$. Model (22) used with parameters as in (35).

the cell density $u(x, y, t)$ and the chemoattractant concentration $v(x, y, t)$ as well as the corresponding vertical profile is shown in Fig. 8.

The simulated vertical distribution of active cells (Fig. 8b) shows two noticeable peaks: one near the top surface and another one near the bottom surface. Two peaks in the vertical cell distribution were also observed experimentally: one at the contact line level, while the other is about 1.5 mm below the contact line [A5]. The position of the simulated peak next to the contact line level differs essentially from that observed experimentally.

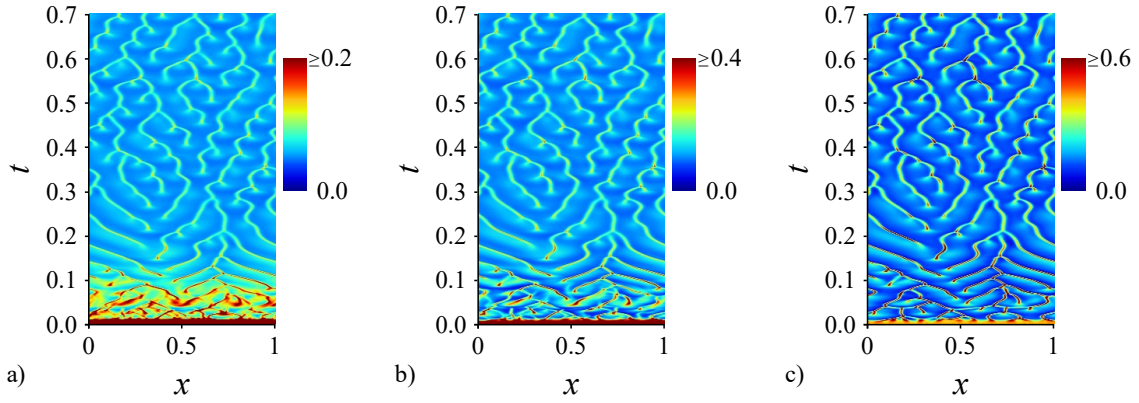

9 pav. Space-time plots of the cell density u_{1D} along the three-phase contact line simulated by using (36) at the following dimensionless parameters: $o_0 = 1.0$, $D_o = 0.12$, $\lambda = 0.048$ and other parameters as in (35), and three heights of the detectable bioluminescence: $h_0 = h$ (a), $h_0 = 0,5h$ (b) ir $h_0 = 0,1h$ (c).

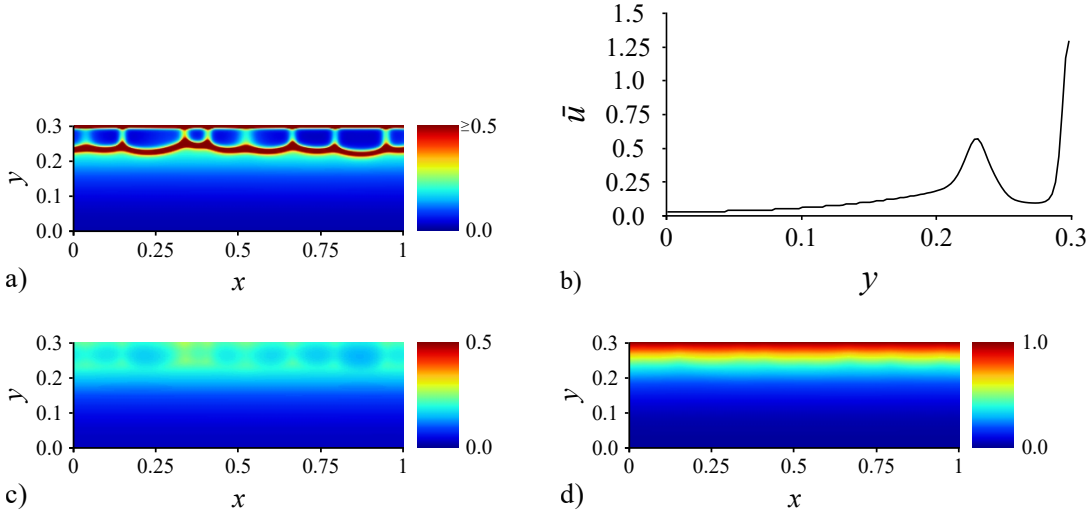

10 pav. Snapshots of the cell density u (a) and the chemoattractant concentration v (c) and oxygen o (d) on the inner lateral surface of the tube and the profile of the vertical distribution of cells (b) at $t = 0.4$. Model used: (23) with the same parameters as in Figure 9.

4.2.2. The case of the resource (oxygen) dependent carrying capacity

The extended model (23) with the introduced oxygen dynamics equation was used for numerical simulations with these additional parameter values: oxygen concentration $o_0 = 1.0$, oxygen diffusivity $D_o = 0.12$ and oxygen consumption rate $\lambda = 0.048$. Obtained simulated patterns can be seen in Fig. 9 and Fig. 10.

As one can see from Fig. 9, the two dimensional model based on the governing

equations (23) can be used for the simulation of the pattern formation along the three-phase contact line assuming different thickness of the experimentally detectable layer. The patterns simulated at different values of the height h_0 are almost identical – only the intensity of the bioluminescence is different. These patterns compare well to the experimentally observed ones when compared subjectively and objectively (according to the values in Table 1).

The simulated 2D plots are also better suited for modelling of experimentally observed ones as peaks of vertical distribution of active cells (Fig. 10b) are at similar depths as experimentally observed.

4.3. Model generalization to two and three dimensions

The aim of this section was to investigate the 3D model of the bacterial self-organization. Since the simulation based on the 3D model is very time-consuming, therefore reducing spatial dimensionality in a model for simulating 1D and 2D spatiotemporal patterns was investigated.

4.3.1. Numerical simulation

The created mathematical model (24) as well as the corresponding dimensionless model (27) were defined as the initial boundary value problems based on a system of nonlinear partial differential equations.

Four special cases were analysed:

1. The 3D model (27).
2. The two-dimensional-in-space of the top surface (2D polar) model (28).
3. The one-dimensional-in-space of the top contact line (1D) model (30).
4. The two-dimensional-in-space of the lateral surface (2D Cartesian coordinates) model (31).

The digital simulator described in Section 3.1 was used.

To simulate spatiotemporal patterns of the quasi-one-dimensional cell density in a vessel near the three-phase contact line by applying the 2D and 3D models, the density u of cells was integrated over the thin range close to the three-phase contact line and then averaged.

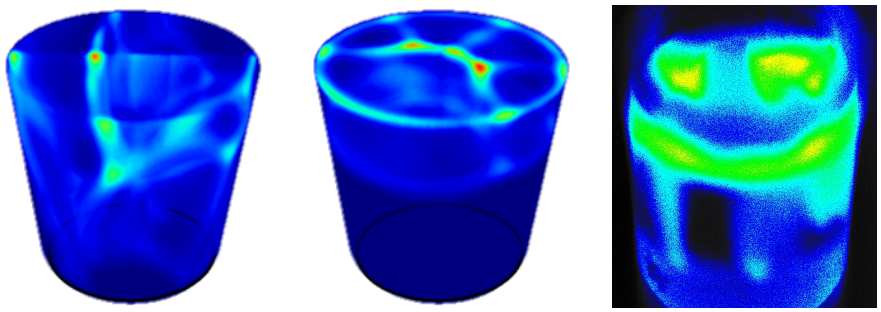

11 pav. Visualization of arbitrary frames at u concentrations obtained by 3D simulation at two time moments: 65 and 329. The snapshot of the experimental culture is shown for comparison [A2].

4.3.2. Results of numerical simulation and discussion

Fig. 12 shows the spatiotemporal patterns of the quasi-one-dimensional cell density simulated by four versions of the model, while Fig. 11 demonstrates a visualization of the arbitrary frames of the cell density when simulating in 3D with the following values of the model parameters:

$$\begin{aligned} D_u = 0.1,\ D_o = 0.2,\ \chi = 8.3,\ \alpha_u = 1,\ \beta_v = 0.73, \\ \gamma_o = 0.025,\ R = 5,\ H = 10,\ \delta = 0.075,\ T = 400. \end{aligned} \tag{37}$$

It can be seen from Fig. 11 that the cell density u inside the rounded container forms foam-like structures similar to the experimentally observed structures [A5, 36]. The simulation results also show (Fig. 12) that the basic spatiotemporal patterns are preserved when the model dimension is reduced: merging and emerging dynamics are present in all four simulations of the pattern formation near the three-phase contact line. On the other hand, the simulated spatiotemporal patterns are not very similar to one another, though the values of the model parameters were the same. The difference in the simulated spatiotemporal patterns could be explained by assumptions used for the reduction of the dimensionality, a relatively large domain size and the sensitivity to the initial conditions.

Since the dimensionless diffusion coefficient D_u and the chemotactic sensitivity χ are the main parameters controlling the mass transport in the 1D model (30), the sensitivity of the spatiotemporal pattern formation to the model parameters D_u and χ was investigated and showed that the modelling error which rose when model dimensionality was reduced can be at least partially compensated by adjusting the values of the D_u and/or χ-parameters.

4.4. Dimensional parameters and their suitability

Taking into account the transformation of the variables ((26) and (32)), the values of the dimensional parameters can be determined.

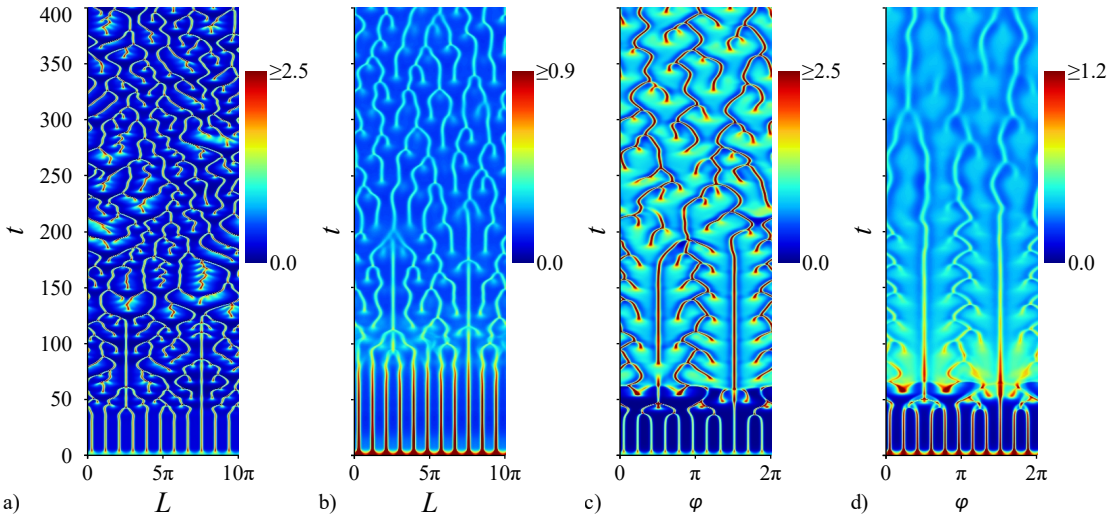

12 pav. Spatiotemporal plots of the dimensionless cell density u for four analysed cases: 1D model (a), 2D model in Cartesian coordinates (b), 2D polar model (c) and 3D model (d). The values of the parameters are as defined in (37).

Analyzing (35) and assuming the length of the contact line ($l = 2\pi R$, where $R \approx 0.3\ cm$ is the radius) and the duration ($T_e = 1.5 \times 10^4\ s = 250\ min$) of the physical experiment corresponds to the dimensionless length ($L = 1$) and the duration ($T = 0.7$), used in the numerical experiments (8), it is possible to calculate other parameter values.

The dimensional diffusion coefficients of the: chemoattractant ($D_c = (l/L)^2 \times (T/T_e) \approx 1.66 \times 10^{-4}\ cm^2 s^{-1}$), the cells ($D_n = D_u D_c = 0.04 D_c \approx 6.63 \times 10^{-6} cm^2 s^{-1}$) and oxygen ($D_s = D_o D_c = 0.12 D_c \approx 1.99 \times 10^{-5} cm^2 s^{-1}$). The corresponding estimations of the diffusion coefficients can be found in the literature [3, 16]: $D_c \approx 10^{-5}\ cm^2 s^{-1}$, $D_n \approx 6 \times 10^{-6}\ cm^2 s^{-1}$ and $D_s \approx 2.0 \times 10^{-5}\ cm^2 s^{-1}$. The possible interpretation of a very large value of the diffusion coefficient of the attractant is presented in [A5].

The dimensional cell growth rate of cells in the model is $0.028\ s^{-1}$, which means that the cell division period equals to $ln(2)/0.028 \approx 25\ s$. The value of the cell division period differs from the typical numerical value of the cell doubling time (about 104 s) about four times, can be explained by the metabolic flexibility of *E. coli* [35].

The dimensional consumption rate of oxygen equals to about 2.8×10^6 molecules per active cell per second and is typical of the metabolically active bacteria in a nutrient rich media [26].

Conclusions

1. Constant chemotactic sensitivity, local sampling, linear gradient and linear diffusion of cells can be successfully used to model the pattern formation in a luminous *E. coli* colony. The effect of the non-local sampling can be partly compensated by using the nonlinear diffusion of cells. Similarly, the effect of the nonlinear gradient can also be partly compensated by using the nonlinear diffusion of cells. Because of this, the selected minimal model is suitable for modelling pattern formation in a luminous *E. coli* colony in pseudo-one dimension along the three-phase contact line.

2. The proposed novel mathematical and computational models with the added equation describing oxygen dynamics become more suitable for modelling a pattern formation in a luminous *E. coli* colony in two and three dimensions of space while considering a vessel with depth compared to analogous models without oxygen dynamics equation.

3. Although a rounded container is best represented by the 3D model, due to the accumulation of luminous cells near the three-phase contact line, the experimental spatiotemporal patterns of the bioluminescence can also be qualitatively simulated by using 1D and 2D models. Nevertheless, important differences in the shape of the patterns are observed between the 1D, 2D and 3D cases when the same values of the model parameters are used in the simulations. Very similar spatiotemporal patterns of the bioluminescence can be simulated using mathematical models of different dimensionality by adjusting the values of the model parameters, particularly of the dimensionless diffusion coefficient and/or chemotactic sensitivity.

Publications on the thesis topic

[A1] R. Baronas, Ž. Ledas, and R. Šimkus. Computational modeling of self-organization in a liquid phase bacterial bioluminescent biosensor. *Proceedings of the 6th European Congress on Computational Methods in Applied Sciences and Engineering (ECCOMAS 2012)*. Ed. by J. Eberhardsteiner et al. Vienna: Vienna University of Technology, 2012, Paper ID: 4815.

[A2] R. Baronas, Ž. Ledas, and R. Šimkus. Computational modeling of the bacterial self-organization in a rounded container: the effect of dimensionality. *Nonlinear Anal. Model. Control* 20(4), 2015, pp. 603–620.

[A3] R. Baronas, Ž. Ledas, and R. Šimkus. Modeling and Simulation of Bacterial Self-Organization in Circular Container Along Contact Line as Detected by Bioluminescence Imaging. *IARIA International Journal on Advances in Systems and Measurements* 5(3&4), 2012, pp. 154–163.

[A4] Ž. Ledas, R. Baronas, and R. Šimkus. Švytinčių bakterijų struktūros cilindrinio mėgintuvėlio šoniniame paviršiuje kompiuterinis modeliavimas. *Computational Science and Techniques* 1(2), 2013, pp. 103–111.

[A5] R. Šimkus, R. Baronas, and Ž. Ledas. A multi-cellular network of metabolically active *E. coli* as a weak gel of living Janus particles. *Soft Matter* 9(17), 2013, pp. 4489–4500.

[A6] R. Šimkus, R. Meškienė, Ž. Ledas, R. Baronas, and R. Meškys. Microtiter plate tests for segregation of bioluminescent bacteria. *Luminescence* 31(1), 2016, pp. 127–134.

References

[1] R. Baronas and R. Šimkus. Modeling the bacterial self-organization in a circular container along the contact line as detected by bioluminescence imaging. *Nonlinear Anal. Model. Control* 16(3), 2011, pp. 270–282.

[2] S. Blackman. *Beginning 3D Game Development with Unity 4: All-in-one, multi-platform game development*. Berkely: Apress, 2013.

[3] M. P. Brenner, L. S. Levitov, and E. O. Budrene. Physical mechanisms for chemotactic pattern formation by bacteria. *Biophys. J.* 74(4), 1998, pp. 1677–1693.

[4] E. O. Budrene and H. C. Berg. Dynamics of formation of symmetrical patterns by chemotactic bacteria. *Nature* 376(6535), 1995, pp. 49–53.

[5] M. van Canneyt, M. Gärtner, S. Heinig, F. Monteiro de Cavalho, and I. Ouedraogo. *Lazarus – the Complete Guide*. Netherlands: Blaise Pascal Magazine, 2011.

[6] M. E. Cates, D. Marenduzzo, I. Pagonabarraga, and J. Tailleur. Arrested phase separation in reproducing bacteria creates a generic route to pattern formation. *PNAS* 107(26), 2010, pp. 11715–11720.

[7] R. Čiegis. *Diferencialinių lygčių skaitiniai sprendimo metodai*. Vilnius: Technika, 2003.

[8] R. Čiegis. *Lygiagretieji algoritmai ir tinklinės technologijos*. Vilnius: Technika, 2005.

[9] R. Čiegis and A. Bugajev. Numerical approximation of one model of bacterial self-organization. *Nonlinear Anal. Model. Control* 17(3), 2012, pp. 253–270.

[10] S. Daunert, G. Barrett, J. S. Feliciano, R. S. Shetty, S. Shrestha, and W. Smith-Spencer. Genetically engineered whole-cell sensing systems: coupling biological recognition with reporter genes. *Chem. Rev.* 100(7), 2000, pp. 2705–2738.

[11] D. Dormann and C. J. Weijer. Chemotactic cell movement during Dictyostelium development and gastrulation. *Curr. Opin. Genet. Dev.* 16(4), 2006, pp. 367–373.

[12] M. Eisenbach. *Chemotaxis*. London: Imperial College Press, 2004.

[13] M. B. Gu, R. J. Mitchell, and B. C. Kim. Whole-cell-based biosensors for environmental biomonitoring and application. *Adv. Biochem. Eng. Biotechnol.* 87, 2004, pp. 269–305.

[14] T. Hillen and K. J. Painter. A user's guide to PDE models for chemotaxis. *J. Math. Biol.* 58(1-2), 2009, pp. 183–217.

[15] T. Hillen, K. Painter, and C. Schmeiser. Global existence for chemotaxis with finite sampling radius. *Discr. Cont. Dyn. Syst. B* 7(1), 2007, pp. 125–144.

[16] A. J. Hillesdon, T. J. Pedley, and O. Kessler. The development of concentration gradients in a suspension of chemotactic bacteria. *Bull. Math. Bio.* 57, 1995, pp. 299–344.

[17] B. P. Ingalls. *Mathematical Modeling in Systems Biology*. USA: MIT Press, 2013.

[18] E. F. Keller and L. A. Segel. Model for chemotaxis. *J. Theor. Biol.* 30(2), 1971, pp. 225–234.

[19] E. F. Keller and L. A. Segel. Travelling bands of chemotactic bacteria: A theoretical analysis. *J. Theor. Biol.* 30(2), 1971, pp. 235–248.

[20] R. Kowalczyk. Preventing blow-up in a chemotaxis model. *J. Math. Anal. Appl.* 305(2), 2005, pp. 566–588.

[21] B. Kvedaras and M. Sapagovas. *Skaičiavimo metodai*. Vilnius: Mintis, 1974.

[22] I. R. Lapidus and R. Schiller. Model for the chemotactic response of a bacterial population. *Biophys. J.* 16(7), 1976, pp. 779–789.

[23] S. Leestma and L. Nyhoff. *Pascal Programming and Problem Solving*. Fourth. New York: Prentice Hall, 1993.

[24] Y. Lei, W. Chen, and A. Mulchandani. Microbial biosensors. *Anal. Chim. Acta* 568(1-2), 2006, pp. 200–210.

[25] P. K. Maini, M. R. Myerscough, K. H. Winters, and J. D. Murray. Bifurcating spatially heterogeneous solutions in a chemotaxis model for biological pattern generation. *Bull. Math. Biol.* 53(5), 1991, pp. 701–719.

[26] D. S. Martin. The oxygen consumption of Escherichia coli during the lag and logarithmic phases of growth. *J. Gen. Physiol.* 15(6), 1932, pp. 691–708.

[27] J. D. Murray. *Mathematical Biology: II. Spatial Models and Biomedical Applications, 3rd ed.* Berlin: Springer, 2003.

[28] M. R. Myerscough, P. K. Maini, and K. J. Painter. Pattern formation in a generalized chemotactic model. *Bull. Math. Biol.* 60(1), 1998, pp. 1–26.

[29] K. J. Painter and T. Hillen. Spatio-temporal chaos in a chemotactic model. *Physica D* 240(4-5), 2011, pp. 363–375.

[30] K. Painter and T. Hillen. Volume-filling and quorum-sensing in models for chemosensitive movement. *Can. Appl. Math. Quart.* 10(4), 2002, pp. 501–543.

[31] H. T. Park, J. Wu, and Y. Rao. Molecular control of neuronalmigration. *Bioessays* 24(9), 2002, pp. 821–827.

[32] A. A. Samarskii. *The Theory of Difference Schemes*. New York-Basel: Marcel Dekker, 2001.

[33] H. Shoji, M. Nonomura, and K. Yamada. Three-dimensional specific patterns based on the Keller-Segel model. *Forma* 27(1), 2012, pp. 19–23.

[34] R. Šimkus. Bioluminescent monitoring of turbulent bioconvection. *Luminescence* 21(2), 2006, pp. 77–80.

[35] R. Šimkus and R. Baronas. Metabolic self-organization of bioluminescent *Escherichia coli*. *Luminescence* 26(6), 2011, pp. 716–721.

[36] R. Šimkus, V. Kirejev, R. Meškienė, and R. Meškys. Torus generated by *Escherichia coli*. *Exp. Fluids* 46(2), 2009, pp. 365–369.

[37] J. Stenhammar, D. Marenduzzo, R. J. Allen, and M. E. Cates. Phase behaviour of active Brownian particles: the role of dimensionality. *Soft Matter* 10(10), 2014, pp. 1489–1499.

[38] M. J. Tindall, P. K. Maini, S. L. Porter, and J. P. Armitage. Overview of mathematical approaches used to model bacterial chemotaxis II: Bacterial populations. *Bull. Math. Biol.* 70(6), 2008, pp. 1570–1607.

[39] J. J. L. Velazquez. Point dynamics for a singular limit of the Keller-Segel model. I. Motion of the concentration regions. *SIAM J. Appl. Math.* 64(4), 2004, pp. 1198–1223.

[40] B. Wilkinson and M. Allen. *Parallel Programming: Techniques and Applications Using Networked Workstations and Parallel Computers (2nd Edition)*. Pearson, 2004.

[41] T. C. Williams. *Chemotaxis: Types, Clinical Significance, and Mathematical Models*. New York: Nova Science, 2011.

About the author

Žilvinas Ledas was born in Vilnius, on 3 February 1986. In 2004, he graduated from Vilnius Rytas secondary school (cum laude), and in 2004–2010 obtained software engineering science bachelor and master degrees from Vilnius University (both cum laude). In 2011–2015, he carried out doctoral studies at Vilnius University. Since 2009, Ledas has been working at Vilnius University as a lecturer. Currently, he is giving "Video Game Design and Development" lectures. Since 2014 he has been working as a researcher at Vilnius University Institute of Biochemistry.

What is more, Žilvinas Ledas is a co-founder of UAB Tag of Joy (*www.tagofjoy.lt*), an award winning game development company. He is also a co-founder of the Lithuanian Game Developers Association (*www.lzka.lt*) and acted as a chairman of the board from 2014 to 2015.

KOMPIUTERINIS ŠVYTINČIŲJŲ BAKTERIJŲ STRUKTŪROS FORMAVIMOSI TIRPALE MODELIAVIMAS

Tyrimų sritis ir problemos aktualumas

Įvairūs mikroorganizmai reaguoja į cheminę aplinką. Jie gali jausti įvairias chemines medžiagas ir judėti link arba nuo jų. Toks kryptingas mikroorganizmų judėjimas, priklausantis nuo cheminių gradientų, vadinamas chemotaksiu [12]. Šis procesas yra svarbus ir mikroskopinėms bakterijoms, ir dideliems žinduoliams – daugelio organizmų išlikimas priklauso nuo jų gebėjimo judėti sudėtingomis sąlygomis, nes toks judėjimas daro įtaką daugeliui elgsenos aspektų, pavyzdžiui, maisto šaltinių paieškai, plėšrūnų išvengimui ar poros pritraukimui [14]. Nors chemotaksis pasireiškia daugelyje bakterijų, *Escherichia coli* (žarninė lazdelė) yra viena iš daugiausia tyrinėjamų. Matuodamos per tam tikrą laiką pajaustą vidutinį chemoatraktanto kiekį, bakterijos, tokios kaip *E. coli*, gali valdyti tiesaus judėjimo ir sukimosi fazių kaitą ir taip judėti pageidaujama kryptimi.

E. coli ir daugelis kitų bakterijų pasižymi tuo, kad esant tam tikroms sąlygoms formuoja įvairius struktūrizuotus raštus [3, 27], t. y. bakterijų populiacija terpėje pasiskirsto netolygiai. Pastaraisiais metais buvo stebėtos nedidelėje su oru besiliečiančioje talpoje patalpintų švytinčiųjų *lux* genais žymėtų *E. coli* bakterijų bėgant laikui besikeičiančios erdvinės struktūros [36]. Tačiau kokie tiksliai dėsniai nusako šių struktūrų susidarymą bei kitimą, vis dar nėra aišku.

Per paskutinius keliolika metų ši bakterijų savybė buvo pradėta naudoti konstruojant efektyvius visos ląstelės (angl. *whole-cell*) liuminescencinius biojutiklius, kurie gali būti taikomi, pavyzdžiui, aplinkoje esantiems teršalams aptikti [13]. Dėl to svarbu aiškintis ir tirti bakterijų judėjimą ir struktūrų susidarymą lemiančius bei valdančius veiksnius.

Matematinių modelių taikymas leidžia patvirtinti biologinių stebėjimų rezultatus retrospektyviai bei kurti naujas hipotezes. Tačiau modeliai dažnai būna sudėtingi, t. y. nagrinėjamos lygtys yra netiesinės, tad iš esmės vienintelis tinkamas būdas jas išspręsti yra naudojant skaitinius metodus [32].

Darbo tikslas ir uždaviniai

Darbo tikslas – sudaryti lankstų bakterijų populiacijos struktūros formavimosi kompiuterinį modelį, tinkamai aprašantį realių eksperimentų rezultatus ir, taikant sudarytą modelį, ištirti bakterijų populiacijos struktūros dinamikos dėsningumus.

Disertacijos tikslui įgyvendinti buvo suformuluotos tokios užduotys:

1. Sudaryti kuo paprastesniais reiškiniais užrašomą, bet pakankamai lankstų bakterijų populiacijos struktūros formavimosi kompiuterinį modelį (remiantis Hillen ir Painter [14], toliau darbe vadinamas „minimaliu“).
2. Matematiškai modeliuoti deguonies poveikį bakterijų populiacijos struktūros formavimuisi.
3. Modelį suderinti su realių eksperimentų rezultatais.
4. Bakterijų populiacijos struktūros formavimosi modelį pritaikyti dvimatei ir trimatei erdvėms bei gauti ir išanalizuoti skaitinio modeliavimo rezultatus vienmatėje, dvimatėje bei trimatėje erdvėse.
5. Sukurti įrankius (programinę įrangą), palengvinančius švytinčiųjų bakterijų vaizdų apdorojimą, jų struktūros analizę bei vizualizavimą.
6. Naudojant sukurtą programinę įrangą, išanalizuoti modeliuotų bei eksperimentinių struktūrų savybes ir elgseną.

Tyrimo metodai

Šiame darbe formuluojami matematiniai modeliai paremti netiesinių diferencialinių lygčių dalinėmis išvestinėmis sistemomis, aprašančiomis bakterijų, chemoatraktanto bei deguonies koncentracijų dinamiką. Lygčių sistemos buvo sprendžiamos skaitiniais metodais. Panaudotas išreikštinių baigtinių skirtumų metodas, įgyvendintas *Free Pascal* programavimo kalba. Modeliai buvo formuluojami vienmatėje (1D), dvimatėje (2D) ir trimatėje (3D) erdvėse.

Taip pat buvo sukurti programiniai įrankiai, palengvinantys švytinčiųjų bakterijų vaizdų apdorojimą, jų struktūros analizę bei vizualizavimą. Įgyvendinant apdorojimo ir analizės įrankių funkcijas, buvo naudojami skaitmeninių vaizdų apdorojimo metodai, siekiant patogiai vizualizuoti 3D erdvėje, buvo panaudotos kompiuterinių žaidimų variklio funkcijos.

Sukurti įrankiai panaudoti modeliams ir parinktiems parametrams patvirtinti pagal realių eksperimentų duomenis, lyginant bakterijų kolonijų formuojamų darinių skaičius bei jų kaitą.

Darbo mokslinis naujumas

1. Parinktas minimalus modelis, tinkantis *E. coli* formuojamoms švytinčiosioms struktūroms modeliuoti pseudovienoje dimensijoje prie mėgintuvėlyje esančio skysčio trijų fazių (kietas paviršius-oras-skystis) kontakto linijos.
2. Sudarytas matematinis ir kompiuterinis modeliai, tinkantys modeliuoti *E. coli* formuojamas švytinčiąsias struktūras dviejų ir trijų dimensijų srityse. Į modelį įtraukta deguonies koncentracijos dinamiką aprašanti lygtis užtikrina, kad

gautos modeliuotos struktūros geriau atitinka matomas realių eksperimentų vaizduose.

3. Nustatyta, kad kintantys erdvėje ir laike struktūrų vaizdai gali būti kokybiškai modeliuojami naudojant mažiau dimensijų (t. y. imant 1D ir 2D modelius), tačiau kartu parodyta, kad atsiranda svarbių raštų skirtumų imant tas pačias parametrų reikšmes skirtingų dimensijų modeliuose.

Darbo rezultatų praktinė reikšmė

Šiame darbe pristatomi matematiniai modeliai yra taikomi aprašyti realiuose eksperimentuose fiksuojamus švytinčiųjų *E. coli* bakterijų formuojamus vaizdus. Tokių matematinių modelių kompiuterinis įgyvendinimas padeda analizuoti bakterijų elgsenos subtilybes, kurių neįmanoma arba yra ypač sunku aiškintis kitaip.

Darbo metu buvo sukurta programinė įranga:

1. Matematinius modelius įgyvendinanti programinė įranga, skirta bakterijų elgsenai tirti.
2. „*E. Coli* Image Analysis“ programinė įranga[3], skirta modeliuotų ir realių eksperimentų vaizdų apdorojimui, analizei ir palyginimui.
3. 3D modeliavimo rezultatams vizualizuoti pritaikytas kompiuterinių žaidimų variklis *Unity* (versija 4.6).

Disertacijos rengimo metu gauti rezultatai buvo panaudoti įgyvendinant mokslinį projektą, „*E. coli* ir jos mutantų saviorganizacija prie trijų fazių kontakto linijos“ finansuojamą Lietuvos mokslo tarybos (MIP-001/2014).

Ginamieji teiginiai

1. Parinktas minimalus modelis yra tinkamas *E. coli* formuojamoms švytinčiosioms struktūroms modeliuoti pseudovienoje dimensijoje prie mėgintuvėlyje esančio skysčio trijų fazių (kietas paviršius-oras-skystis) kontakto linijos.
2. Įtraukus deguonies koncentracijos dinamiką aprašančią lygtį sudarytas matematinis ir kompiuterinis modeliai yra tinkami modeliuoti *E. coli* formuojamas švytinčiąsias struktūras dviejų ir trijų dimensijų erdvėse, kai modeliuojama visame mėgintuvėlyje esančiame skystyje.
3. Kintantys erdvėje ir laike bakterijų formuojamų struktūrų vaizdai gali būti kokybiškai modeliuojami naudojant modelius, turinčius mažiau dimensijų, tačiau tada atsiranda svarbių raštų skirtumų naudojant tas pačias parametrų reikšmes skirtingų dimensijų modeliuose.

[3] Ją galima rasti adresu: http://uosis.mif.vu.lt/~zledas/bakt/ImageAnalysis/.

Darbo rezultatų aprobavimas

Pagrindiniai tyrimų rezultatai buvo publikuoti 5 straipsniuose periodiniuose mokslo leidiniuose [A2–A6]. Trys iš jų [A2, A5, A6] yra publikuoti referuojamuose ir turinčiuose citavimo rodiklį Thomson Reuters (ISI) duomenų bazėje Web of Science žurnaluose. Šios disertacijos autorius dalyvavo visuose publikacijų rengimo etapuose, bet daugiausiai prisidėjo prie skaitinio modelio rengimo ir skaitinių skaičiavimų rezultatų gavimo bei apdorojimo. Taip pat dalis mokslinių rezultatų buvo publikuota recenzuojamame mokslinės konferencijos leidinyje [A1]. Tyrimų rezultatai pristatyti ir aptarti 7 nacionalinėse ir tarptautinėse konferencijose.

Bendrosios išvados

1. Konstantinė chemotaktinio jautrio funkcija, vietinis jautris, tiesinis gradientas ir tiesinė difuzija gali būti sėkmingai taikomi švytinčiųjų *E. coli* bakterijų kolonijos formuojamiems raštams modeliuoti. Nevietinio gradiento įtaka bakterijų formuojamiems raštams gali būti iš dalies kompensuota įtraukus netiesinę ląstelių difuziją. Panašiai netiesinio gradiento poveikis gali būti iš dalies kompensuojamas įtraukiant netiesinę ląstelių difuziją. Atsižvelgiant į tai, parinktas modelis, darbe vadinamas minimaliu, yra tinkamas švytinčiųjų *E. coli* bakterijų formuojamoms struktūroms modeliuoti pseudovienoje dimensijoje prie mėgintuvėlyje esančio skysčio trijų fazių (kietas paviršius-oras-skystis) kontakto linijos.

2. Pasiūlyti nauji matematinis ir kompiuterinis modeliai, kuriuose atsižvelgiama į deguonies koncentracijos dinamiką, yra tinkamesni švytinčiųjų *E. coli* bakterijų formuojamoms struktūroms modeliuoti dviejų ir trijų dimensijų erdvėse, kai atsižvelgiama į bakterijų judėjimą per visą mėgintuvėlio gylį, palyginti su analogiškais modeliais be deguonies dinamiką aprašančios lygties.

3. Bakterijų populiacijos dinamikai cilindro formos mėgintuvėlyje esančiame skystyje modeliuoti geriausiai tinka 3D modelis. Vis dėlto didesnės bakterijų koncentracijos formuojasi palei viršutinio cilindro paviršiaus kraštą, dėl to kintantys erdvėje ir laike raštai gali būti kokybiškai modeliuojami naudojant 1D ir 2D modelius. Tačiau atsiranda svarbių raštų skirtumų taikant 1D, 2D ir 3D modelius su tomis pačiomis parametrų reikšmėmis. Labai panašūs erdvėje ir laike kintantys švytinčiųjų bakterijų formuojami raštai gali būti modeliuojami taikant skirtingų dimensijų modelius ir pritaikant dalies parametrų reikšmes, konkrečiai bedimensį bakterijų difuzijos koeficientą ir (arba) chemotaktinį jautrį.

Žilvinas Ledas

COMPUTATIONAL MODELLING OF THE SELF-ORGANIZATION OF LUMINOUS BACTERIA IN LIQUID

Summary of doctoral dissertation

Physical sciences, informatics (09 P)

Editor Zuzana Šiušaitė

Žilvinas Ledas

KOMPIUTERINIS ŠVYTINČIŲJŲ BAKTERIJŲ STRUKTŪROS FORMAVIMOSI TIRPALE MODELIAVIMAS

Daktaro disertacijos santrauka

Fiziniai mokslai, informatika (09 P)

Redaktorė Eglė Bukienė